Journal of Sustainability Science and Management
Volume 18 Number 12, December 2023: 43-55
eISSN: 2672-7226

THE SATELLITE DERIVATION OF DEPTH AND TOTAL SUSPENDED SOLIDS ASSESSMENT FOR ESTUARINE EROSION MONITORING WITHIN NARROW STRAIT USING SENTINEL-2A SATELLITE IMAGES

HASHIM SITI SYAFIQAH[1], AZIZ KHAIRUL NAIM ABD.[1]*, ROSLEE AME AZMAN[1], TAJAM JAMIL[1], ROSLANI MUHAMMAD AKMAL[1], KAMARUDDIN SHARIR AIZAT[1] AND MOHD FAZLY AMRI[2]

[1]Marine Research Station (MARES), Faculty of Applied Sciences, Universiti Teknologi MARA, Perlis Branch, Arau Campus, 02600 Arau, Perlis, Malaysia. [2]Faculty of Architecture, Planning and Surveying, Universiti Teknologi MARA Cawangan Perlis Branch, Arau Campus, 02600 Arau, Perlis, Malaysia.

**Corresponding author: khairul567@gmail.com*
Submitted final draft: 30 March 2023 *Accepted: 2 May 2023* http://doi.org/10.46754/jssm.2023.12.005

Abstract: Estuaries are crucial marine areas for important hydrodynamics processes, such as sediment transport for supporting other marine ecosystems like mangrove forests. This study explores the relationship between total suspended solids (TSS) and water depth within a narrow strait area with Sentinel-2A satellite images. The gravimetric method and Normalise Suspended Material Index (NSMI) were used for TSS analysis and estimations. In contrast, the bathymetric survey and Stumpf ratio transform were used to validate and estimate the water depth from the satellite images. The estimation process begins with an assessment using 2018 in-situ data and further analysis of the differences between 2018 and 2020 using Sentinel-2A image comparison. This study found a relatively moderate estimation between water depth and satellite imagery at 53%, and the TSS estimation results show a stronger relationship of up to 80% as they were both analysed separately. The relationship between TSS and water depth shows a solid connection, which explains the correlation of 75-82% between them by the satellite images. The strong connection of estimation for depth and TSS within the narrow strait suggests continuous monitoring is reliable to support decisions for immediate action at estuarine areas.

Keywords: Sustainability, remote sensing, total suspended solids, satellite derived bathymetry, Sentinel-2A.

Introduction

Estuaries are bodies of water that connect land and sea, extending from an entirely marine environment to the effective limit of tidal influence and where seawater is diluted by freshwater inflow. Estuaries also serve as nurseries for a variety of species, provide habitat for a diverse range of organisms for all or part of their life cycles, and are known for their high biological production (ELTurk *et al.,* 2019). Moreover, this marine area is a unique feature of coastal zones and is among the most developed and utilised regions (Azhikodan & Yokoyama, 2021). Within estuaries, asymmetries in tidal propagation exist, impacting sediment movement throughout the river-estuary-ocean continuum (Asp *et al.*, 2018). These variations in movement made the sediment easier to trap within the estuary (Geyer & Ralston, 2018). Some estuaries contain mangrove areas, which are coastal vegetation that grows in muddy tidal environments. The mangrove forest is a type of tropical and subtropical forest that grows near the coast or on a river that is subject to tides. Because mangroves play a vital role as a natural water filtering system, these areas are increasingly protected as authorities realise how important these systems are (Pahlevan *et al.*, 2017). The mangrove forest brings significant benefits, particularly in coastal areas and coastal communities. Moreover, the mangrove ecosystem plays an important role in protecting coastal and river areas from erosion (Le Nguyen & Luong, 2019).

In protecting these areas, remote sensing has been used to continuously monitor them over the last few years. Remote sensing is the

science and art of obtaining information about an object, location or phenomenon by evaluating data obtained using devices that are not in direct contact with the object (Jégat *et al.,* 2016). Large global coverage, high spatial resolution, high revisit frequency and low cost are among the advantages of satellite remote sensing techniques over traditional field sampling methods (Hedley *et al.*, 2018). It is the ultimate support for traditional surveys, especially in areas that are difficult to reach (Hodúl *et al.,* 2018; Li *et al*., 2019).

Through the analysis of satellite data, researchers have discovered that changes in hydrodynamics will influence benthic environments. Some studies have been carried out on a large scale using the satellite Sentinel-2A for hydrodynamic observation (Wachid *et al.*, 2017; Hedley *et al.*, 2018; Wang & Atkinson, 2018). The entire value of mineral and organic material, including sediments transported in suspension by an estuary channel, is referred to as total suspended solids (TSS). The sediment movement in the water is linked to ongoing physical, chemical and biological processes (Dai *et al.*, 2018). These processes occur naturally and have reached equilibrium over ages until humans are over-interacted with the environment. Anthropogenic activity has influenced the estuary and exposed it to erosion and deposition of sediment flow in the water that will affect the marine ecosystem (de Souza Machado *et al.*, 2016).

Continuously monitoring the changes would require high cost and time for gathering in-situ samples and observations. Thus, estimations and predictions are used to forecast these changes using satellite images, which this study refers to as satellite derived TSS (SDTSS). Remote sensing can provide novel approaches for quantifying TSS concentrations in surface water. Satellites can be used to monitor water quality by relating solar radiation reflected from the water body, as measured by a sensor aboard the satellite, to a water quality parameter (Isidro *et al.*, 2018). In estuarine areas, anthropogenic activities, and environmental stressors (de Souza Machado, 2016; Azhikodan & Yokoyama, 2021) are known to be the main factors that impose negative effects on sediment flow. Various studies have proven that monitoring these changes takes time and effort; thus, remote sensing techniques are one of the keys to tackling the issue (Jégat *et al.*, 2016; Chen *et al.*, 2021; Westley, 2021). Multispectral imaging is the most utilised data for satellite derived bathymetry (SDB) (Westley, 2021). The availability of newer, high-resolution Sentinel satellite (Sentinel-2A) images has great potential (Wang & Atkinson, 2018) and has been used to estimate water depth or SDB (Caballero & Stumpf, 2019).

However, an integration of analyses utilising the SDB and SDTSS from these newer satellite images that are expected to improve sedimentation monitoring systems has not been well addressed. This study aims to explore the use of Sentinel-2A satellite images for water depth and TSS derivation to monitor the sediment flow, erosion, and status of the estuarine area around the Langkawi Islands. Satellite images captured by satellite spectral sensors are one of the space-borne remote sensing approaches expected to improve monitoring capability (Chen *et al.*, 2021).

In order to achieve that, two objectives have been outlined which include determining the applicability of the SDB and SDTSS estimation by Sentinel-2A satellite images with respect to in-situ data and analysing their correlation for sedimentation monitoring capabilities. The findings of this study hopefully will improve the sedimentation forecast and analysis, with the integration of satellite-derived information for depth and TSS, especially in the estuarine areas of Langkawi.

Materials and Methods

Study Area

The Bagan Nyior Strait, located at 6°16’ N, 99°50’ E (Figure 1), a narrow estuarine channel, is one of the major routes to Pulau Tuba and Pulau Dayang Bunting, Langkawi. Year after year, Langkawi attracts many visitors across the globe. Tourism Malaysia, in collaboration with

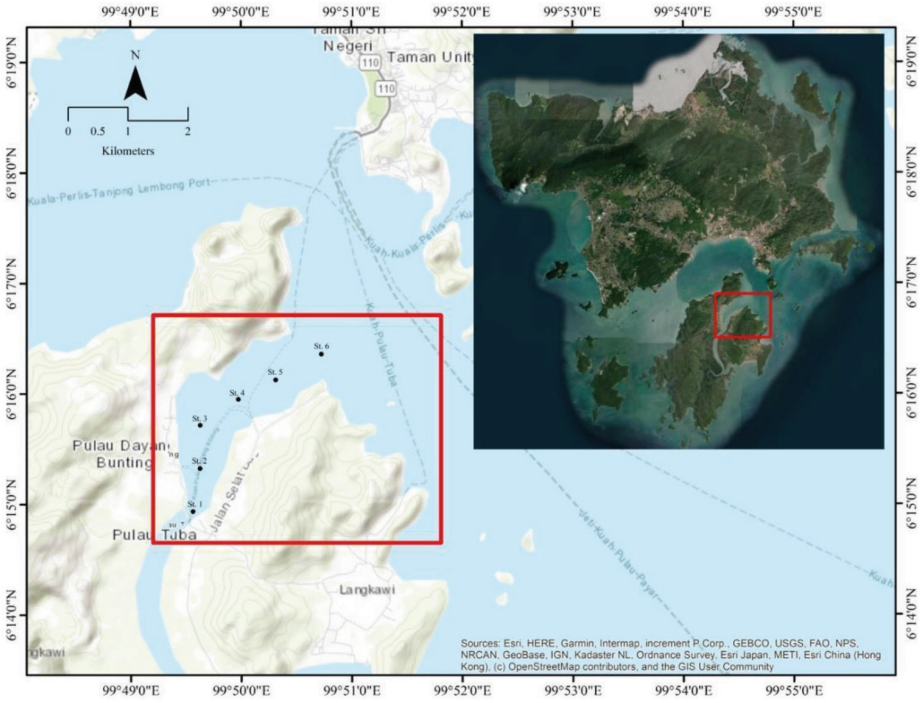

Figure 1: The study area in the narrow channel estuary of Bagan Nyior strait, off Pulau Langkawi, with in-situ points for data acquisition

the local government, particularly the Langkawi Development Authority (LADA), is committed to promoting the island and developing it as a tourist destination. Recently, the island has proven to be one of Malaysia's greatest vacation destinations. In-situ data acquired was related to TSS collected in October 2018 and processed using the gravimetric method. Most of the stations were located in the middle of the strait, with only one station (St.3) located near the arch-shaped area. The overall workflow of this study is visualised in a flow chart (Figure 2).

Satellite Data and Pre-Processing

This study utilised Sentinel-2A images from 2018 and 2020 that covered the study area, having less than 10% cloud cover. Images from Sentinel-2A were obtained via Sentinel's Scientific Data Hub (https://scihub.copernicus.eu/). These images correspond to a pre-processed Level-2A (L2A) product, where they were radio-metrically and geometrically corrected. With a spatial resolution of 10, 20, and 60 m, the MSI sensor aboard the Sentinel-2A satellites monitors the Earth's reflected radiation in 13 spectral bands, from visible to NIR and SWIR (Drusch *et al.*, 2012). The information about the MSI bands and their spatial resolution is shown in Table 1. The in-situ TSS data was used to build up a comparison to the remotely sensed data from satellite images as TSS was generated from satellite images based on an algorithm developed Arisanty and Saputra (2017), while the depth value retrieved from SDB (Caballero & Stumpf, 2019) was generated based on reference data from the previous survey.

Before any algorithms were used for processing and estimation, the Sentinel-2A images were resampled and atmospherically corrected. In resampling, all images from various bands were sharpened to 10 m spatial resolution in advance (Punalekar *et al.*, 2018) and subset to the study area's water bodies (land masked). As the data processing was limited to water territory, the sun de-glinting method was used to smoothen any waves and curve reflections

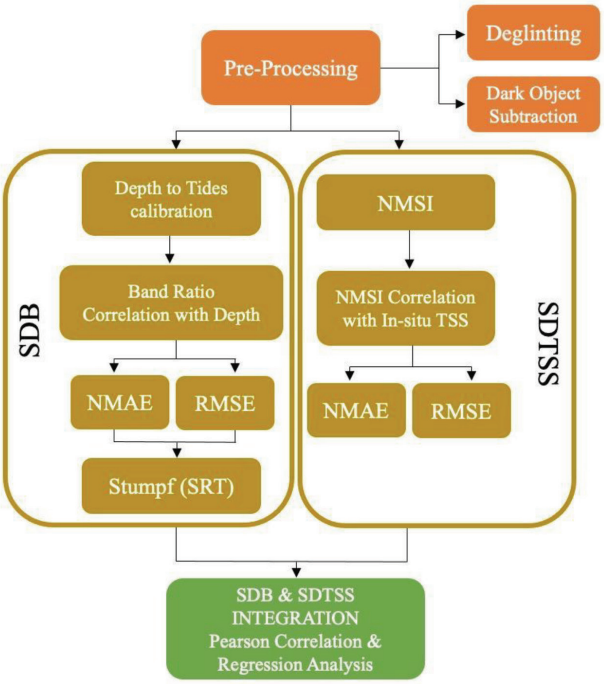

Figure 2: The workflow of the SDB and SDTSS integration which includes pre-processing, processing and the integration analysis of both in remotely sensed approaches

Table 1: The band's specifications of spatial resolution (SR), central wavelength (CW) and bandwidth (BW) of the Sentinel-2 image. [Adapted from The European Space Agency (2021)]

Acronym	Band	SR (m)	CW (nm)	BW (nm)
B1	Violet	60	443	20
B2	Blue	10	490	65
B3	Green	10	560	35
B4	Red	10	665	30
B5	Red-edge 1	20	705	15
B6	Red-edge 2	20	740	15
B7	Red-edge 3	20	783	20
B8	NIR	10	842	115
B8A	NIR narrow	20	865	20
B9	NIR	60	945	20
B10	NIR	60	1375	30
B11	SWIR1	20	1610	90
B12	SWIR2	20	2190	180

(Hedley *et al.*, 2018). A previous study had suggested frequent acquisition of images that clearly cover the study area, however, very few clear images that are close to the date were available. After that, dark-object subtraction (DOS) was also applied (Mondejar & Tongco, 2019) to the related bands for image correction (Figure 3).

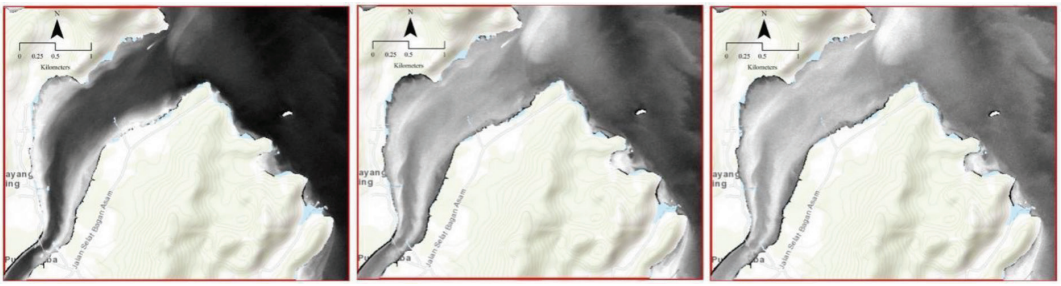

(a) (b) (c)

Figure 3: The effect of the geometric and atmospheric correction to the satellite images for (a) Red, (b) Green and (c) Blue bands from Sentinel-2A satellite

Satellite Image Processing (SDB)

A nonlinear solution based on a band ratio calculation is a common method for obtaining bathymetry from satellite imagery (Caballero & Stumpf, 2019). The ratio between bands is essentially generated by the varying levels of absorption, and this ratio will change concurrently as the depth changes. Theoretically, when the ratio rises, the depth will rise with it and the band with a higher level of absorption will continue to decrease (Said *et al.*, 2017). This study used the Stumpf Ratio Transform (SRT) method to generate the study area bathymetric map as in Equation 1.

$$Z = m_1 \left[\frac{ln\ nR_w(\lambda i)}{ln\ nR_w(\lambda j)}\right] - m_0 \qquad (1)$$

where, Z is the calculated depth (in metres), m_1 is the constant coefficient from the ratio relationship while m_o is its constant coefficient when depth is at zero, *n* is a constant multiplier (normally 1000), $R_w(\lambda i)$ is the remote sensing reflectance of the blue band and $R_w(\lambda j)$ is the remote sensing reflectance of the green band. The application of this method needs the calibration of measured depth from the onsite survey, and this study took advantage of previous sounding corrected and tides calibrated bathymetric data nearest to the strait opening, which was at Tanjung Pandan, Pulau Tuba in 2018 (Figure 4).

Satellite Image Processing (SDTSS)

The TSS recording and monitoring, on the other hand, is a difficult operation since these tiny particles (often between 0.062 and 2 mm) lose their connection to the bottom due to their flow and movement with the current (Ghaderi & Rahbani, 2021). However, the combination of remote sensing and modelling can be a

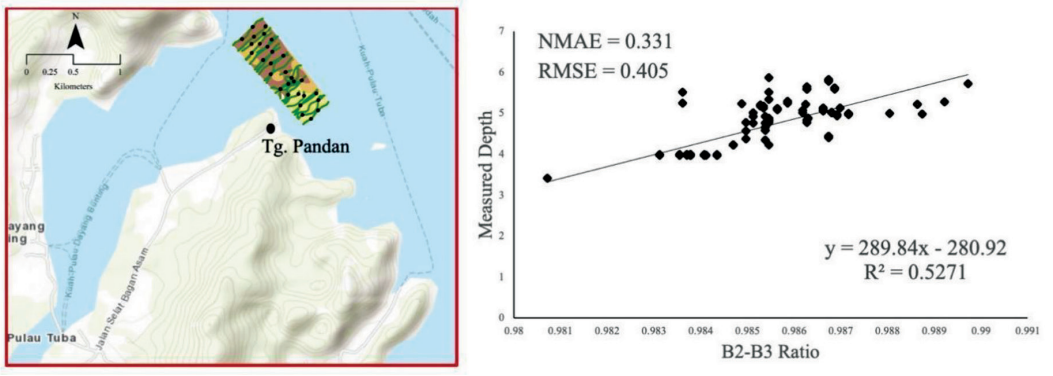

Figure 4: The application of the Stumpf ratio method utilising (a) in-situ depth with 100 validation points to produce relationship ratio equation from (b) depth to Blue-Green band (B2-B3) where the constants are used for depth estimation

major tool for enhancing suspended sediment forecasts in this research area and contributing to greater confidence in the modelling of various management scenarios. Moreover, the use of a transition model based on MSI Sentinel-2A with a Normalised Suspended Material Index (NSMI) technique (Arisanty & Saputra, 2017) effectively captures complex spatiotemporal TSS patterns in the study area for SDTSS estimation. The TSS concentrations were identified from water turbidity within the study area and evaluated against in-situ data recorded using the gravimetric method at six sample stations along the Bagan Nyior strait (Figure 5).

The NSMI was applied in this study to calculate TSS concentration (Equation 2). The NSMI is based on the fact that clear water has a peak reflectance in the blue band, whereas suspended material promotes an increase in reflectance throughout the visible spectrum, particularly in the green and red bands (red + green band), where clear water tends to absorb radiation (Ghaderi & Rahbani, 2021).

The performance of NSMI and SRT (Figure 4 to 5) was assessed using Normalised Mean Absolute Error (NMAE) (Equation 3) and Root Mean Square Error (RMSE) (Equation 4). The NMAE was used to determine the error between the estimate and observed values. The RMSE was used to get the difference between the estimated and observed values. The RMSE value obtained must be close to zero to indicate a small error in the in-situ (Casal *et al.*, 2019).

$$NSMI = \frac{(Red\ Band)+(Green\ Band)-(Blue\ band)}{(Red\ band)+(Green\ band)+(Blue\ band)} \quad (2)$$

$$NMAE = \sum_{i=1}^{n} |x_{satellite} - x_{insitu}| \quad (3)$$

$$RMSE = \sqrt{\frac{\sum_{i=1}^{n} (x_{satellite}-x_{insitu})^2}{n}} \quad (4)$$

where, $X_{satellite}$ represents concentration of TSS from remote sensed measurements, X_{insitu} represents concentration of TSS from the in-situ measurements and n represents number of sample stations.

Data Analysis

The TSS data from in-situ measurement and processed satellite images were analysed, and the results were used to establish the relationship between measured and remotely sensed estimation for TSS. The estimation and differences for each year of 2018 and 2020 were portrayed in graphs to determine the relationship between depth and TSS within the study area, and finally, their degree of relationship was identified using a linear regression method. In assessing the performance of integration of TSS and depth for sediment analysis at the estuary area, the regression model was carried out to find the significant relationship between both variables using correlation and regression analyses. The Pearson Correlation (r) value (Equation 5) was analysed to find the correlation between the two variables and to determine whether the relationship between them was weak or strong, while coefficient determination

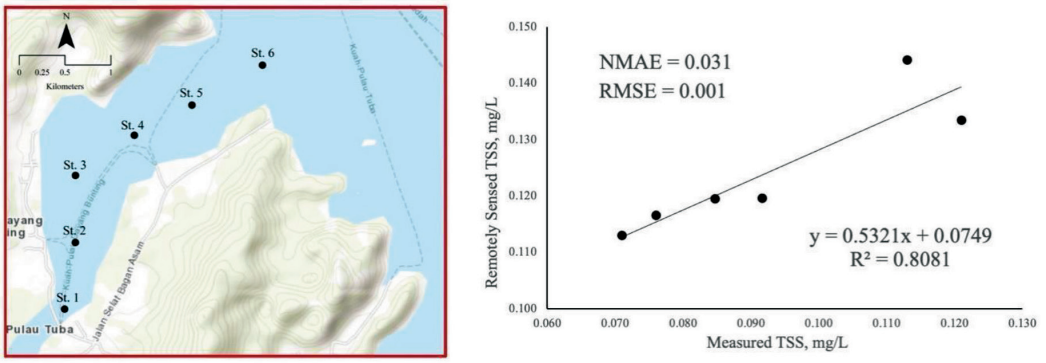

Figure 5: The application of the Normalised Suspended Material Index (NSMI) method utilising (a) in-situ TSS with 6 validation stations, to test the applicability of estimation by analysing their (b) correlation errors

(R^2) (Equation 6), in the linear regression was used to show the proportion of variance that explained the changes between variables that are interdependent. The greater the R^2 value, the better the algorithm's performance fit.

$$r = \frac{n\sum [(X_{satellite} - X_{insitu})] - [(\sum X_{insitu})(\sum X_{satellite})]}{\sqrt{[n(\sum X_{satellite}{}^2) - (\sum X_{satellite})^2] \cdot [n(\sum X_{insitu}{}^2) - (\sum X_{insitu})^2]}} \quad (5)$$

$$Coefficient\ Determination\ (R^2) = (Correlation\ Coefficient)^2 \quad (6)$$

where, $X_{satellite}$ represents concentration of TSS from remote sensed measurements, X_{insitu} represents concentration of TSS from the in-situ measurements and n represents the number of sample stations.

Results and Discussion

Satellite Derived Bathymetry (SDB)

SDB may refer to a variety of approaches that determine water depths using space-based sensors (Westley, 2021). In this study, the ability of Sentinel-2A imagery to map a bathymetry surface by using the SRT method at 10 m spatial resolution over shallow optical regions was successfully demonstrated (Figure 5). SDB mapping at 10 m has a number of advantages, including the ability to retrieve more features (Casal *et al.*, 2019), especially in areas with complex geomorphological features, such as narrow channels. Overall, the bathymetric map at Bagan Nyior strait for 2018 shows a lower depth estimation compared to the 2020 depth, with an average reading of 4.09 and 4.65 m respectively (Table 2).

The greatest contrast in depth is at St.1 even though it was expected to be the shallowest in 2018 and 2020 at 2.23 and 4.05 m respectively, with a range of 1.82 m making it the biggest change of depth of all the stations. Depth underestimation at the St.1 area in 2018 was caused by a cloud shadow coverage in the image, which disrupted the depth estimation in that area (Figure 6). Unexpectedly, the St.6 point showed the least depth changes where it recorded the lowest range of -0.10 m, even though the station was among the deepest, from 4.95 m in 2018 and reduced to 4.85 m in 2020. Due to the constant in and out-flow of sediments at the estuary opening (Kanga *et al.*, 2020), significant changes were expected to be obvious at the St.6 point.

Satellite Derived Total Suspended Solids (SDTSS)

Comparing remotely sensed data with in-situ data shows that high quality products can be obtained from remotely sensed data because it provides qualitative and quantitative analysis of remote sensing reflection products (Pahlevan

Table 2: The differences in water depths and TSS concentrations at six stations in Bagan Nyior strait between 2018 and 2020

Station	TSS (mg/L)			Depth (m)		
	2018	2020	Difference	2018	2020	Difference
1	0.1573	0.1196	-0.038	2.226	4.050	+1.824
2	0.1674	0.1195	-0.048	3.861	4.439	+0.578
3	0.1797	0.1166	-0.063	4.098	4.279	+0.180
4	0.1839	0.1441	-0.040	4.336	5.674	+1.338
5	0.1822	0.1129	-0.069	5.044	4.596	-0.448
6	0.1937	0.1334	-0.060	4.954	4.850	-0.104

*Note: The positive values indicate increment and negative values indicate decrement.

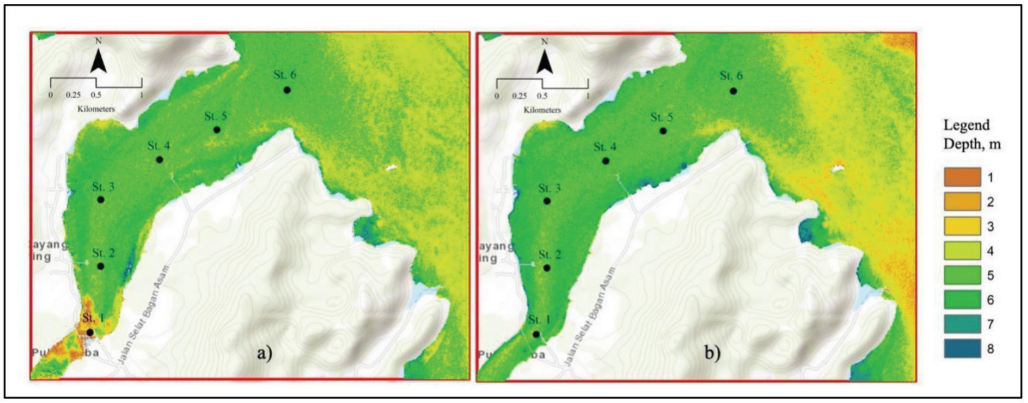

Figure 6: The application of Normalised Suspended Material Index (NSMI) method utilising (a) in-situ TSS with 6 validation stations, to test the applicability of estimation by analysing their (b) correlation errors

et al., 2017). The values extracted from the process found a strong relationship of TSS from Sentinel-2A images which are about 80% in R^2 and lower NMAE and RMSE with 0.031 and 0.001 respectively (Figure 5). The TSS values derived from satellite images were overestimated on average at all stations for both 2018 (0.177 mg/L) and 2020 (0.124 mg/L) predictions (Table 3). While Figure 7 shows the SDTSS concentration within the study area with slight changes in TSS distribution pattern, an obvious change occurred just beyond the strait area between 2018 and 2020. The greatest TSS change found was at St.5, where TSS concentration had reduced by 0.069 mg/L from 2018 to 2020 with predicted values between 0.1822 and 0.1129 mg/L respectively.

Another station that should be weighed up is St.3, which shows a reduction of 0.063 mg/L and has the second highest in TSS difference notwithstanding the station in the arch area. This may be due to construction activities during those years, such as jetties' maintenance, resorts and chalets, that influenced the TSS through construction materials affecting water turbidity. The effects of land use are essentially the effects of human activities (human activities that take place on land area) on water quality (Chen *et al.*, 2021). High turbidity with contamination could lead to less light penetration to the seafloor, which could potentially disturb the plankton and other benthic organisms in the area (ELTurk *et al.*, 2019).

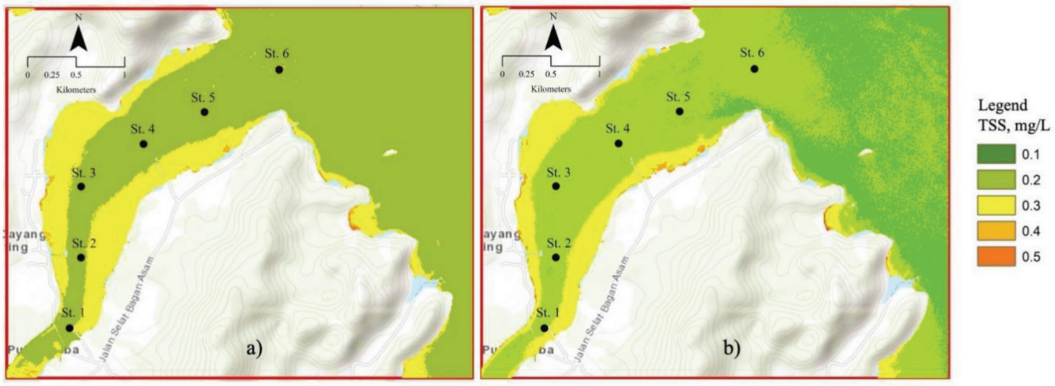

Figure 7: The estimation of TSS within the area of study in (a) 2018 and (b) 2020 by using the transition method of NSMI for SDTSS at Bagan Nyior strait

Mangrove forests in estuaries play an important role in protecting the shoreline and river from erosion, thus reducing any sediment from entering the waters (Le Nguyen & Luong, 2019). However, the concentration of TSS at the water and land boundaries (riverbank) has been estimated to be above average in both years, indicating that the riverbanks were affected the most compared to the middle of the strait. Moreover, the sediment loss from the riverbanks was visually observed on both sides of the strait between 2018 and 2020 with a clear difference in band 8 of the NIR wavelength (Figure 8). The NIR band is usually used for land masking, thus it could effectively be used to separate water from land, this is because water absorbs more energy from NIR wavelength compared to land areas (Mondejar & Tongco, 2019). Syahreza *et al.* (2012) and Isidro *et al.* (2018) stated that, at lower TSS concentrations, the spectral signature of water contains a peak surface reflectance between the green and red bands, whereas, at greater TSS concentrations, the peak moves towards the near-infrared band or longer wavelengths.

The Relationship of SDB and SDTSS

In order to integrate the TSS and depth estimation into sedimentation analysis in this study, the relationship between both predicted values of the SDB and SDTSS must be examined. As the study focuses on how the change of each parameter affects one another, the main task is to see whether any changes in depth could affect the TSS value in the water bodies. Figure 9 shows the correlation and regression analysis of both parameters to test their applicability. The output obtained (Figure 9) for the coefficient of determination, R^2 was

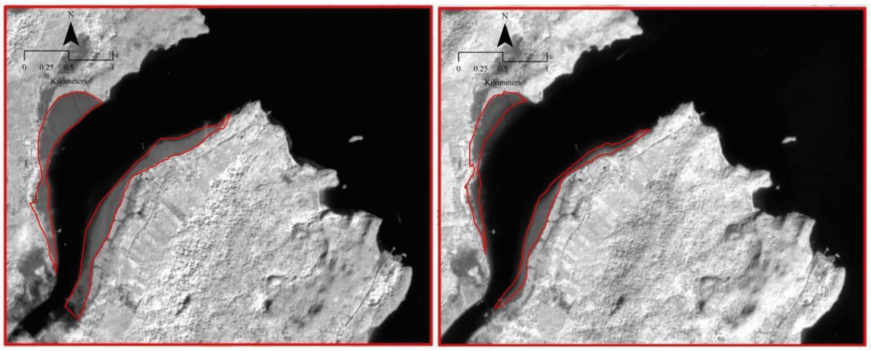

Figure 8: The changes at riverbanks from band 8 in the NIR images between (a) 2018 and (b) 2020 visually indicate a loss of sediment that could contribute to the TSS within the Bagan Nyior strait

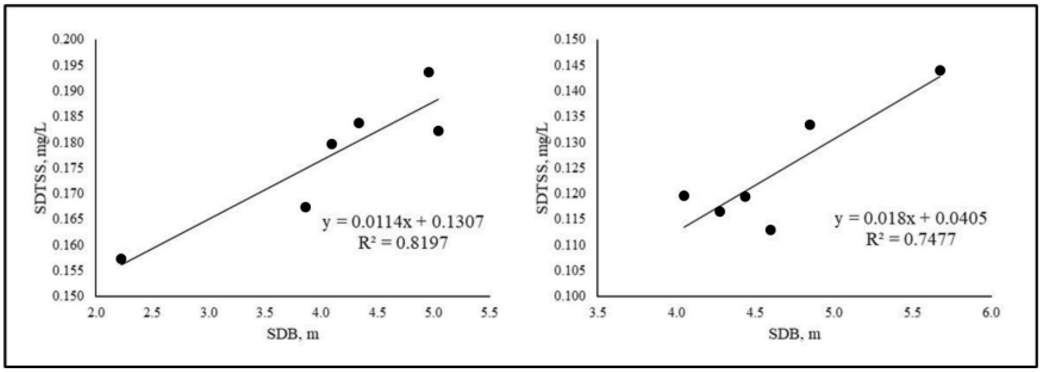

Figure 9: The correlation and regression analysis between SDB and SDTSS for both years (a) 2018 and (b) 2020 to verify their integration applicability to monitor sediment within the water body of Bagan Nyior strait

about 82% in 2018 and about 75% in 2020 which indicates a positive sign of integrating both depth and TSS parameters in the analysis. The remaining 18-25% could be influenced by other factors such as turbulence within the tidal harmonics range, wind waves and swells, watershed inflow, climatic variability and human activities, such as deforestation, agriculture, and urbanisation, which are all known to influence changes in sedimentation distribution (Nguyen *et al.*, 2020). The estimation from satellite images and analysis between both parameters are related significantly with a *P*-value of lower than 0.05 and a very small standard error between 0.0027 and 0.0052 in 2018 and 2020 respectively (Table 3).

By comparing the two years (2018 and 2020) of estimation from Sentinel-2A, this study was able to analyse the differences across the two parameters. The changes in depth and TSS within the two years are obtained by subtracting the 2020 from previous the 2018 value. The values were obtained from the processed images at six stations along the Bagan Nyior strait. Overall, the changes of TSS in the strait were reduced by an average of 0.053 mg/L, and the depth increased by an average of 0.56 m between the two years. The analysis from Table 2 and graphs plotted in Figure 10 showed a gradual increment of TSS from St.1 to St.6 in 2018 but fluctuated in 2020 which resulted to an inconsistency of TSS differences over those years. The same pattern also extends to depth distributions between 2018 and 2020, however, cloud shadow over St.1 did disturb the depth estimation of that station.

Table 3: The correlation and regression analysis on the SDB and SDTSS during 2018 and 2020 for their integration applicability toward the sediment monitoring system

Year	*P* value	Std Error	r	R^2
2018	0.0130, < 0.05	0.0027	+0.9054	0.8197
2020	0.0262, < 0.05	0.0052	+0.8647	0.7477

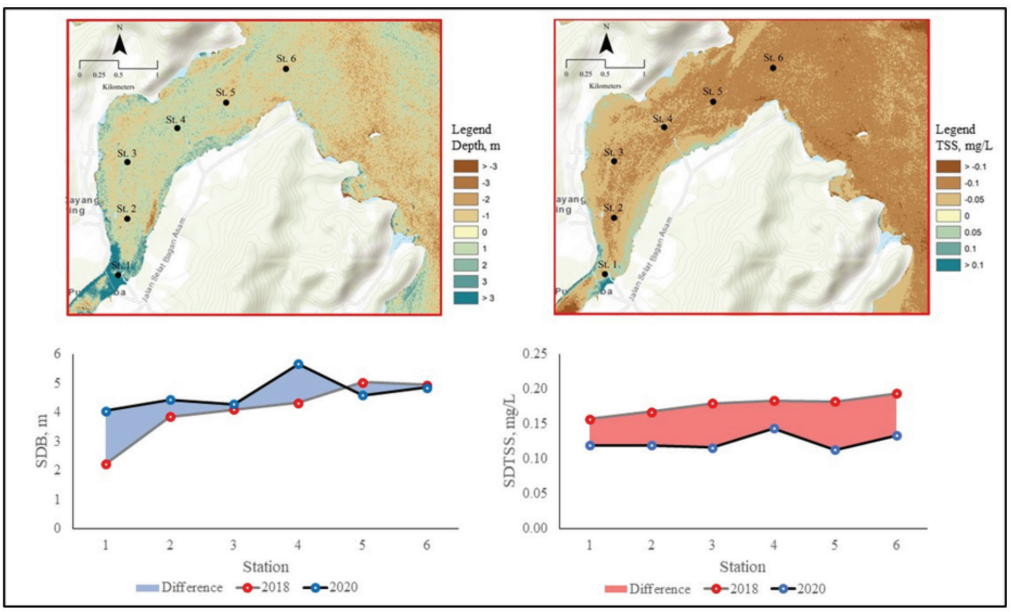

Figure 10: The changes of (a) depth and (b) TSS after the estimation process within two years of 2020 to 2018 and the graphs of differences for comparison of (c) depth and (d) TSS along the six stations at Bagan Nyior

Sediment is the most common component in the water column, both in terms of weight and volume. The sediment from the estuarine area would extend kilometres beyond the coastal areas, and other than the coastal current regulation, the sediment transport is also driven by buoyancy and/or wind, and can also be trapped on the shoreline (Deng *et al.*, 2017). Aside from natural events, human intervention across the strait was the main contributor to landscape changes, TSS variations and depth (Eulie *et al.*, 2018). While acquiring in-situ data at the station in 2018, we observed jetty maintenance (St.4), tourism activities such as chalets and restaurants (St.2) and floating hotels in progress (St.1). However, in 2020 all stations showed a decline pattern in TSS. This may be due to fewer human activities during the COVID-19 pandemic. From these observations, this study has found that depth differences and TSS concentrations do have a relationship with anthropogenic activities, and these activities can affect the condition of the strait if not managed properly in line with sustainable development practices.

Conclusion

In many ways, continuous data collection and monitoring for environmental studies is difficult, particularly in terms of cost and time. Utilising satellite images helps reduce the cost of surveys in the field. This study proposed an estuarine monitoring technique by evaluating the potential integration of depth and suspended sediments analysis by using Sentinel-2A satellite images, which will improve the environmental studies within that region. Employing SRT and NSMI techniques to the Sentinel-2A satellite images for depth and TSS estimation has proven that both are reliable independently with a great correlation between remotely sensed and in-situ data. This study had also shown that the integration between SDB and SDTSS was strong with a correlation coefficient of 75% to 82% after the analyses had been carried out. Therefore, integrating SDB and SDTSS is one of the reliable techniques for sedimentation monitoring in estuarine areas. As this is a new adaptation to the field, it is suggested that increased frequency and widened coverage of in-situ monitoring in the coming years so that the estimation of this integration analysis could achieve higher precision and accuracy. The integration of SDB and SDTSS analysis, could improve the monitoring of estuarine areas and assist stakeholders for conservation and sustainable development planning in the future.

Acknowledgements

This research was supported by the Ministry of Higher Education (MoHE) of Malaysia through the Fundamental Research Grant Scheme (FRGS/1/2021/WAB05/UITM/03/2). We also want to thank Universiti Teknologi MARA (UiTM) for research support through the SDG Triangle Lestari Grant [600-RMC/LESTARI SDG-T 5/3 (002/2021)].

References

Arisanty, D., & Saputra, A. N. (2017). Remote sensing studies of suspended sediment concentration variation in Barito Delta. *IOP Conference Series: Earth and Environmental Science* (Vol. 98, No. 1, p. 012058). IOP Publishing.

Asp, N. E., Gomes, V. J. C., Schettini, C. A. F., Souza-Filho, P. W. M., Siegle, E., Ogston, A. S., & Queiroz, M. C. (2018). Sediment dynamics of a tropical tide-dominated estuary: Turbidity maximum, mangroves and the role of the Amazon River sediment load. *Estuarine, Coastal and Shelf Science*, *214*, 10-24.

Azhikodan, G., & Yokoyama, K. (2021). Erosion and sedimentation pattern of fine sediments and its physical characteristics in a macrotidal estuary. *Science of the Total Environment*, *753*, 142025.

Caballero, I., & Stumpf, R. P. (2019). Retrieval of nearshore bathymetry from Sentinel-2A and 2B satellites in South Florida coastal waters. *Estuarine, Coastal and Shelf Science*, *226*, 106277.

Casal, G., Monteys, X., Hedley, J., Harris, P., Cahalane, C., & McCarthy, T. (2019). Assessment of empirical algorithms for bathymetry extraction using Sentinel-2 data. *International Journal of Remote Sensing*, *40*(8), 2855-2879.

Chen, W., Wang, J., Cao, X., Ran, H., Teng, D., Chen, J., & Zheng, X. (2021). Possibility of using multiscale normalized difference vegetation index data for the assessment of total suspended solids (TSS) concentrations in surface water: A specific case of scale issues in remote sensing. *Environmental Research*, *194*, 110636.

Dai, Z., Mei, X., Darby, S. E., Lou, Y., & Li, W. (2018). Fluvial sediment transfer in the Changjiang (Yangtze) river-estuary depositional system. *Journal of Hydrology*, *566*, 719-734.

Deng, B., Wu, H., Yang, S., & Zhang, J. (2017). Longshore suspended sediment transport and its implications for submarine erosion off the Yangtze River Estuary. *Estuarine, Coastal and Shelf Science*, *190*, 1-10.

de Souza Machado, A. A., Spencer, K., Kloas, W., Toffolon, M., & Zarfl, C. (2016). Metal fate and effects in estuaries: A review and conceptual model for better understanding of toxicity. *Science of the Total Environment*, *541*, 268-281.

Drusch, M., Del Bello, U., Carlier, S., Colin, O., Fernandez, V., Gascon, F., & Bargellini, P. (2012). Sentinel-2: ESA's optical high-resolution mission for GMES operational services. *Remote sensing of Environment*, *120*, 25-36.

ELTurk, M., Abdullah, R., Zakaria, R. M., & Bakar, N. K. A. (2019). Heavy metal contamination in mangrove sediments in Klang estuary, Malaysia: Implication of risk assessment. *Estuarine, Coastal and Shelf Science*, *226*, 106266.

Eulie, D. O., Corbett, D. R., & Walsh, J. P. (2018). Shoreline erosion and decadal sediment accumulation in the Tar-Pamlico estuary, North Carolina, USA: A source-to-sink analysis. *Estuarine, Coastal and Shelf Science*, *202*, 246-258.

Geyer, W. R., & Ralston, D. K. (2018). A mobile pool of contaminated sediment in the Penobscot Estuary, Maine, USA. *Science of the Total Environment*, *612*, 694-707.

Ghaderi, D., & Rahbani, M. (2021). Tracing suspended matter in Tiab estuary applying ANN and Remote sensing. *Regional Studies in Marine Science*, *44*, 101788.

Hedley, J. D., Roelfsema, C., Brando, V., Giardino, C., Kutser, T., Phinn, S., & Koetz, B. (2018). Coral reef applications of Sentinel-2: Coverage, characteristics, bathymetry and benthic mapping with comparison to Landsat 8. *Remote sensing of environment*, *216*, 598-614.

Hodúl, M., Bird, S., Knudby, A., & Chénier, R. (2018). Satellite derived photogrammetric bathymetry. *ISPRS journal of photogrammetry and remote sensing*, *142*, 268-277.

Isidro, C. M., McIntyre, N., Lechner, A. M., & Callow, I. (2018). Quantifying suspended solids in small rivers using satellite data. *Science of the Total Environment*, *634*, 1554-1562.

Jégat, V., Pe'eri, S., Freire, R., Klemm, A., & Nyberg, J. (2016, May). Satellite-derived bathymetry: Performance and production. In *Proceedings of the Canadian Hydrographic Conference, Halifax, NS, Canada* (pp. 16-19).

Le Nguyen, H. T., & Luong, H. P. V. (2019). Erosion and deposition processes from field experiments of hydrodynamics in the coastal mangrove area of Can Gio, Vietnam. *Oceanologia*, *61*(2), 252-264.

Li, P., Ke, Y., Bai, J., Zhang, S., Chen, M., & Zhou, D. (2019). Spatiotemporal dynamics of suspended particulate matter in the Yellow River Estuary, China during the past two decades based on time-series Landsat and Sentinel-2 data. *Marine Pollution Bulletin*, *149*, 110518.

Kanga, S., Meraj, G., Das, B., Farooq, M., Chaudhuri, S., & Singh, S. K. (2020). Modelling the spatial pattern of sediment flow in lower Hugli estuary, West Bengal, India by quantifying Suspended Sediment Concentration (SSC) and depth conditions using geoinformatics. *Applied Computing and Geosciences*, *8*, 100043.

Li, Y., Li, C., & Li, X. (2017). Remote sensing studies of suspended sediment concentration variations in a coastal bay during the passages of atmospheric cold fronts. *IEEE Journal of Selected Topics in Applied Earth Observations and Remote Sensing*, *10*(6), 2608-2622.

Mondejar, J. P., & Tongco, A. F. (2019). Near infrared band of Landsat 8 as water index: a case study around Cordova and Lapu-Lapu City, Cebu, Philippines. *Sustainable Environment Research*, *29*(1), 1-15.

Nguyen, T. H. D., Phan, K. D., Nguyen, H. T. T., Tran, S. N., Tran, T. G., Tran, B. L., & Doan, T. N. (2020). Total suspended solid distribution in Hau River using sentinel 2a satellite imagery. *ISPRS Annals of Photogrammetry, Remote Sensing & Spatial Information Sciences*, *6*.

Pahlevan, N., Sarkar, S., Franz, B. A., Balasubramanian, S. V., & He, J. (2017). Sentinel-2 Multispectral Instrument (MSI) data processing for aquatic science applications: Demonstrations and validations. *Remote sensing of environment*, *201*, 47-56.

Punalekar, S. M., Verhoef, A., Quaife, T. L., Humphries, D., Bermingham, L., & Reynolds, C. K. (2018). Application of Sentinel-2A data for pasture biomass monitoring using a physically based radiative transfer model. *Remote Sensing of Environment*, *218*, 207-220.

Said, N. M., Mahmud, M. R., & Hasan, R. C. (2017). Satellite-derived bathymetry: Accuracy Assessment on depths derivation algorithm for shallow water area. *International Archives of the Photogrammetry, Remote Sensing & Spatial Information Sciences*, *42*.

Syahreza, S., MatJafri, M. Z., Lim, H. S., & Mustapha, M. R. (2012, November). Water quality assessment in Kelantan delta using remote sensing technique. *Electro-optical Remote Sensing, Photonic Technologies, and Applications VI, 8542*, 286-292. SPIE.

The European Space Agency (2021, March 4). *Spatial Resolution*. Sentinel Online. Retrieved from https://sentinels.copernicus.eu/web/sentinel/user-guides/sentinel-2-msi/resolutions/spatial

Wachid, M. N., Hapsara, R. P., Cahyo, R. D., Wahyu, G. N., Syarif, A. M., Umarhadi, D. A., & Widyatmanti, W. (2017, June). Mangrove canopy density analysis using Sentinel-2A imagery satellite data. In *IOP Conference Series: Earth and Environmental Science*, *70*(1), 012020. IOP Publishing.

Wang, Q., & Atkinson, P. M. (2018). Spatio-temporal fusion for daily Sentinel-2 images. *Remote Sensing of Environment*, *204*, 31-42.

Westley, K. (2021). Satellite-derived bathymetry for maritime archaeology: Testing its effectiveness at two ancient harbours in the Eastern Mediterranean. *Journal of Archaeological Science: Reports*, *38*, 103030.